Robust Integrated-Energy Management of Shared Transmission Systems for Renewable Fuels and Refined Oil Considering Decision-Dependent Pressure Drop Uncertainty

Shengshi Wang[a,b], Jingguan Liu[a], Bo Zeng[c], Danji Huang[a,d*], Xiaomeng Ai[a], Shichang Cui[a], Yue Zhou[b], Wei Gan[b], Jiakun Fang[a*], Jinyu Wen[a]

[a] State Key Laboratory of Advanced Electromagnetic Technology, School of Electrical and Electronic Engineering, Huazhong University of Science and Technology, Wuhan 430074, Hubei, China

[b] School of Engineering, Cardiff University, Cardiff CF24 3AA, UK

[c] Department of Industrial Engineering and the Department of Electrical and Computer Engineering, University of Pittsburgh, Pittsburgh, PA, USA

[d] PetroChina ShenZhen New Energy Research Institute Co., Ltd., Shenzhen 518000, Guangdong, China

[*] Corresponding author

E-mail addresses: hdj01@petrochina.com.cn (D.J. Huang); jfa@hust.edu.cn (J.K. Fang)

Abstract

This paper investigates robust integrated-energy management (RIM) of shared transmission systems for renewable fuels and refined oil (STS-RR) considering decision-dependent uncertainty (DDU) in pipeline pressure drop to ensure security and efficiency of system operation. Firstly, the two-stage RIM model in STS-RRs is proposed. Specifically, in the day-ahead pipeline schedule

stage, the integrated-energy management of electric pump operation, multi-batch flow delivery and chemical drag reducer (CDR) injection within STS-RRs is considered to reduce energy consumption and operational costs. In the intraday adjustable operation simulation stage, the uncertainty in pressure drop due to decisional CDR injection concentration and pipeline flow rates is characterized by DDU. Additionally, the adjustable in-station facilities are regulated corresponding to pressure drops within the uncertainty sets. Correspondingly, the solution workflow is proposed to simultaneously handle both decision-independent uncertainty and DDU. Finally, extensive case studies on an illustrative STS-RR and a real-world cross-regional multi-product transmission system in South China validate the effectiveness and scalability of the proposed RIM framework, where a 32.24% energy consumption reduction, a 22.20% economic improvement in total cost and a 26.08% increase in turnover for the illustrative case are achieved. Importantly, the DDU-aware modeling reduces unnecessary conservativeness.

Keywords: Two-stage robust integrated-energy management, shared transmission systems for renewable fuels and refined oil, chemical drag reducer, decision-dependent uncertainty, real-world system case.

Nomenclature

Sets and indices:

$t \in \mathrm{T} = \{1,2 \dots t_{\max}\}$	Set of time points
$b \in \mathrm{B} = \{1,2 \dots b_{\max}\}$	Set of LEP batches
$i \in \mathrm{I} = \{1,2 \dots i_{\max}\}$	Set of stations
$l \in \mathrm{L} = \{1,2 \dots l_{\max}\}$	Set of LEPs
$k_i \in \mathrm{K}_i = \{1,2 \dots k_{i,\max}\}$	Set of the pumps at station i
$n \in N_i = \{1,2 \dots n_{i,\max}\}$	Set of the geometric surrogate polytope facets for the pipeline between stations i and $i+1$

Parameters:

V_i^s	Volumetric coordinate of station i (m^3)
M	A large number used in big-*M* method
V_b^{total}	Total volume of batch b (m^3)
T_t	Length of time-step $(t, t+1)$ (h)
$V_{i,l}^{\text{down}}$	Evaluated demand volume of LEP l at station i (m^3)
$o_{b,l}$	$o_{b,l} = 1$ if and only if batch b carries LEP l
μ	Permitted demand deviation ratio (%)
$Q_{i,\min/\max}^{\text{down}}$	Minimum/maximum download flow rate of station i (m^3/h)
$Q_{i,\min/\max}^{\text{pipe}}$	Minimum/maximum flow rate in the pipeline between stations i and $i+1$ (m^3/h)
$\delta_{i,t}$	Integer indicator for LEPs
P^{feed}	Pressure provided by the feed pump (MPa)
$P_{i,\min/\max}^{\text{in/out}}$	Minimum/maximum inlet/outlet pressure of station i (MPa)
g	Gravitational acceleration (m/s^2)
ρ_l, ρ_b	Density of LEP l and batch b (kg/m^3)
L_i	Length of the pipeline between stations i and $i+1$ (km)
E_i	Elevation of the station i (m)
D_i	Internal diameter of the pipeline between stations i and $i+1$ (m)
μ_b	Kinematic viscosity of batch b (m^2/s)
a_i, b_i	Pressure drop coefficients of the pipeline between stations i and $i+1$
Q_i^{pipe}	Rated flow rate in the pipeline between stations i and $i+1$ (m^3/h)
$a_{k_i}^{\text{pump}}$, $b_{k_i}^{\text{pump}}$, $c_{k_i}^{\text{pump}}$	Pumping head characteristics coefficients of pump k_i
κ	Minimum modulation ratio (%)
$price_{t,i}^{\text{ele}}$	Electricity price at station i in time-step $(t, t+1)$ (¥/kWh)
$price^{\text{chem}}$	CDR price (¥/kg)
$price^{\text{pump}}$	Labor cost for switching pumps (¥)
ρ^{chem}	Density of the injected CDR (kg/m^3)
$\Delta P_{t,i,\min/\max}^{\text{err}}$	Minimum/maximum random variation range of $\Delta P_{t,i}^{\text{err}}$ for the pipelines without CDR injected (MPa)

Continuous variables:

$V_{t,b}^{\text{forward}}$	Forward-end volumetric coordinate of batch b at time point t (m^3)
$V_{t,b}^{\text{backward}}$	Backward-end volumetric coordinate of batch b at time point t (m^3)
$Q_{t,i,b}^{\text{down}}$	Flow rate for station i downloading the LEP from batch b in time-step $(t, t+1)$ (m^3/h)
$Q_{t,i}^{\text{pipe}}$	Flow rate in the pipeline between stations i and $i+1$ in time-step $(t, t+1)$ (m^3/h)
$P_{t,i}^{\text{in/out}}$	Inlet/outlet pressure of station i in time-step $(t, t+1)$ (MPa)

$P_{t,i}^{\text{station}}$	Total pressure provided by the pumps at station i in time-step $(t, t+1)$ (MPa)
P_{t,k_i}^{actu}	Actual pressure provided by pump k_i in time-step $(t, t+1)$ (MPa)
P_{t,k_i}^{head}	Pressure that pump k_i provide when it is turned on in time-step $(t, t+1)$ (MPa)
$P_{t,i}^{\text{drop}}$	Nominal pressure drop along the pipeline between stations i and $i+1$ in time-step $(t, t+1)$ (MPa)
$\Delta P_{t,i}^{\text{err}}$	Pressure drop estimation error in the pipeline between stations i and $i+1$ in time-step $(t, t+1)$ (MPa)
H_{t,k_i}^{mod}	Modulated pumping head of pump k_i in time-step $(t, t+1)$ (m)
H_{t,k_i}^{base}	Base-frequency pumping head of pump k_i in time-step $(t, t+1)$ (m)
$W_{t,i}^{\text{station}}$	Total electric energy consumed by the pumps at station i in time-step $(t, t+1)$ (MWh)
W_{t,k_i}^{actu}	Actual electric energy consumed by pump k_i in time-step $(t, t+1)$ (MWh)
$C_{t,i}^{\text{chem}}$	CDR injection concentration at station i in time-step $(t, t+1)$ (ppm)
$C_{t,i,\min}^{\text{chem}} / C_{t,i,\max}^{\text{chem}}$	Min/max CDR injection concentration at station i in time-step $(t, t+1)$ (ppm)

Binary variables:

$B_{t,i,b}^{\text{exc}}$	$B_{t,i,b}^{\text{exc}} = 1$ if and only if the forward-end of batch b exceeds station i at time point t
$B_{t,i,b}^{\text{bet}}$	$B_{t,i,b}^{\text{bet}} = 1$ if and only if station i is in between the forward-end and backward-end of batch b at time point t
$B_{t,i,b}^{\text{inpipe}}$	$B_{t,i,b}^{\text{inpipe}} = 1$ if and only if the forward-end of batch b is in the pipeline between stations i and $i+1$ in time-step $(t, t+1)$
$B_{t,i}^{\text{down}}$	$B_{t,i}^{\text{down}} = 1$ if and only if station i downloads LEP in time-step $(t, t+1)$
B_{t,k_i}^{pump}	$B_{t,k_i}^{\text{pump}} = 1$ if and only if pump k_i is switched on
$B_{t,k_i}^{\text{switch}}$	$B_{t,k_i}^{\text{switch}} = 1$ if and only if the on-off state of pump k_i is changed.

Abbreviations:

LEP	Liquid energy product
STS-RR	Shared transmission system for renewable fuels and refined oil
CDR	Chemical drag reducer
(R)IM	(Robust) Integrated-energy management
DIU	Decision-independent uncertainty
DDU	Decision-dependent uncertainty
C&CG	Column-and-constraint generation
IS	Initial station
LS	Local station
TS	Terminal station
MP	Master problem

SP	Sub-problem
KKT	Karush-Kuhn-Tucker

1. Introduction

Liquid energy products (LEPs), including renewable fuels, refined oil, etc., comprise more than 50% of the global total final energy consumption [1]. The transportation of these products, particularly for cross-regional transmission, mainly relies on backbone energy infrastructures, the pipeline systems [2, 3]. It is estimated that an approximately 45 TWh of electricity is used by these systems per year [4]. However, their energy saving potential has not been thoroughly exploited, despite its significant implications for industrial sustainability and Net Zero. Additionally, emerging literature points out that LEPs with similar physicochemical properties, particularly for renewable fuels and refined oil, are promising to share the pipeline transmission capacities, leading to the development of shared transmission systems for renewable fuels and refined oil (STS-RRs) [5, 6]. Hence, this paper investigates the energy management of the emerging STS-RRs and aims to accomplish energy consumption and cost reduction for system operators.

The scope of energy management for the STS-RRs typically involves the individual management of flow delivery schedules for LEP batches and then the power consumed by electric pumps [7]. This leads to security issues in system operation, as the flow delivery schedule often lacks consideration of the pumps' hydraulic pressure control [8]. Recently, the joint flow delivery and electric pump scheduling has begun to gain prominence [9]. Herein, the detailed flow rates, batch migration processes and pump energy consumption are coordinated. Note that the chemical drag reducer (CDR) is generally injected into the pipelines at industrial sites to improve the flow hydraulic performance against flow drag, increasing pipeline throughput and reduce costs [10, 11]. Therefore, considering practical factors, the scope of energy management for STS-RRs should be

expanded to the integrated-energy management (IM) [12, 13] of electricity, LEPs and CDR to achieve significant energy savings. Besides, the reduction effect of CDR on pipeline pressure drop is difficult to accurately estimate, and the underlying mechanism remains unclear, significantly threatening the security and economy of pipeline operations [14]. Accordingly, uncertain factors arise in the IM of STS-RRs, further increasing the difficulties of real-world practical operations.

To address these problems, it is imperative to first develop an IM model for STS-RRs considering randomness. This mainly include stochastic optimization model [15], chance-constrained model [16] and robust optimization model [17]. As backbone energy infrastructures are vital to a country's social production, the robust optimization can ensure the safe operation when stochastic variables vary within a given robust uncertainty set [18]. The two-stage robust model can clearly describe the logical occurrence of physical processes and is widely used in the planning and operational levels of industrial systems [19]. Therefore, this paper focuses on developing a two-stage robust integrated-energy management (RIM) model, which aims to pre-arrange flow schedules, electric pump on-off states, and CDR injection concentration. This enhances the system's economic and energy-saving effects under safe operating conditions. It also reduces the need for operators to frequently manually intervene and conduct on-site inspections, thereby improving their daily work efficiency.

An essential part of the two-stage robust model is the characterization of uncertainties [20]. There are two main types of uncertainties. One is the decision-independent uncertainty (DIU), which is exogenously introduced, such as the wind/solar power or traffic flow forecast error in the power systems [21], and the changes in the ambient environment surrounding the pipeline [22]. Herein, the minimum and maximum values of the stochastic variables are utilized to cover practical

scenarios [23]. The other type is decision-dependent uncertainty (DDU), which is endogenously produced [24]. In STS-RRs, it mainly involves the estimation error of pipeline pressure drop affected by CDR injection concentration and pipeline flow rates [25].

In addressing two-stage robust optimization problems, most prior works employ the column-and-constraint generation (C&CG) workflow [26], which has become one of the standard approaches for energy-system applications under DIU. However, due to the involvement of DDU in this paper, it may result in over-conservative results or infeasibility [27]. Essentially, this is because the extracted extreme scenarios of the sub-problem (SP), i.e., the vertices of the DDU set, are no longer fixed in the changeable DDU set along with iterations. Correspondingly, the parametric C&CG algorithm has been proposed as the state of the art approach to address this issue [28, 29]. The idea is that it returns extreme scenario sets to the master problem (MP), which are parameterized by the dual variables in SP extracted from a finite set with fixed vertices independent of the decision variables. It can coverage within acceptable numbers of iterations and finds the optimal solution. Hence, the idea of parametric C&CG algorithm is applied to propose the solution workflow in this paper.

References	Research scope	Uncertainties	Modeling	Algorithms
[3, 7, 9]	LEPs multi-batch flow delivery plan management	N/A	Mixed Integer Linear Programming	Solver software
[4, 30-32]	Electricity management	N/A	Mixed Integer Linear Programming	Solver software
[6, 33]	Electricity management	DIU	Markov decision process	Learning method and solver software
[8]	Joint energy management of electricity and LEPs	N/A	Mixed Integer Linear Programming	Solver software

[34, 35]	Single LEP batch flow delivery plan management	DIU	Distributionally robust chance-constrained optimization model	Solver software
[36]	LEPs multi-batch flow delivery plan management	DIU	Chance-constrained optimization model	Solver software
This paper	Integrated-energy management of electricity, LEPs and CDR	DDU and DIU	Two-stage robust optimization model	Parametric C&CG and solver software

TABLE I Comparison of research on energy management for STS-RRs

Overall, main challenges handled by this paper are threefold. Firstly, how to propose the IM under uncertainty, to extend the existing STS-RR energy management framework and thereby enhance system flexibility. Secondly, how to characterize pipeline pressure drop uncertainty driven by CDR injection and pipeline flow rates. Thirdly, how to solve the resulting model efficiently and stably. Accordingly, the main contributions are summarized as follows, compared with other studies in TABLE I.

1) To the best of our knowledge, the research scope of the energy management problem in STS-RRs is for the first time expanded to IM of electricity, LEPs and CDR with uncertainties for flexibility enhancement. Subsequently, the uncertainty in pressure drop dependent on decisional CDR injection concentration and flow rates is first investigated, which is characterized by DDU. Accordingly, a two-stage RIM framework is proposed, ensuring the security and economic efficiency of STS-RR operation.

2) The two-stage RIM model considering DDU in pipeline pressure drop of STS-RRs is proposed. Herein, the detailed hydraulic characteristics of electric pumps and multi-batch flow processes associated with CDR is considered to reflect practical system behavior. A solution

workflow is proposed based on the state-of-the-art parametric C&CG algorithm, which can handle DDU in the proposed RIM model efficiently and stably. Correspondingly, the infeasibility and convergence criteria, together with economic and security regulation rules, are designed based on duality principle and Karush-Kuhn-Tucker (KKT) conditions to iteratively converge on the optimal solution.

3) Extensive case studies on an illustrative STS-RR and especially a real-world cross-regional multi-product transmission system in South China. Results validate the effectiveness and scalability of the proposed framework. Importantly, the DIU-only baseline shows that DDU modeling can mitigate unnecessary conservativeness induced by static uncertainty sets and thereby improve economic efficiency while maintaining secure transmission, providing actionable guidance for on-site dispatchers.

The rest of the paper is organized as follows. Section 2 describes the basis of STS-RR and problem statement. Section 3 introduce the RIM model considering DDU in pressure drop in STS-RR. Section 4 presents the workflow of the proposed RIM framework with the established model. Section 5 shows the case studies. Finally, conclusions are drawn in Section 6.

2. Problem Description

The practical STS-RRs studied in this paper sequentially delivers several types of LEPs, i.e., renewable fuels and refined oil, in the pipeline, consuming significant amounts of electricity to generate driving force [32]. As shown in Fig. 1, the system mainly comprises five parts, i.e., the initial, local and terminal stations (ISs, LSs and TSs), the connecting pipelines, as well as an energy management processor. Specifically, the IS stores the LEPs in categories and uploads the products through the feeding and transmission pumps. At intervals (e.g., every 24 hours), the LSs evaluate

their demands for the next period. Inside the LSs are the hydraulic-related facilities equipped, including electric pumps for driving the LEPs, advanced meters for measurement, frequency modulators for adjusting pumping head output, LEP storage tanks and CDR injection systems for adding CDR into the LEPs to reduce fluid friction. The TS receives the remaining products at the end of the STS-RR. Moreover, it helps to reduce the surplus pressure in the pipeline for maintaining a stable flow rate. In each station, there are dispatchers and engineers monitoring the system states and implementing safety inspections for secure operation.

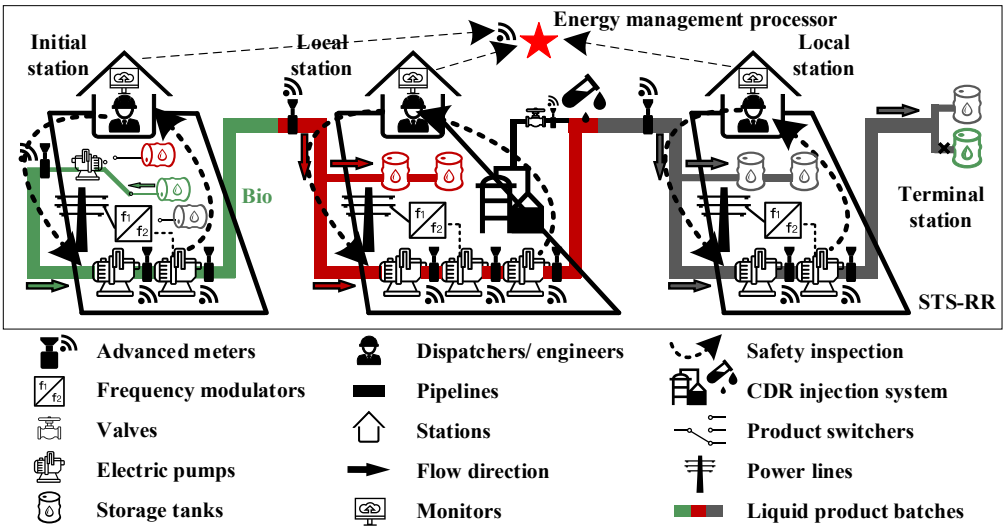

Fig. 1. Schematic diagram of STS-RRs.

Systemically, in the day ahead of the scheduled operation (day-ahead), the energy management processor first gathers the locally evaluated product demands and aggregates them into several batches [31]. In this paper, inspired by the hydraulic equations, i.e., the Pascal's law and Darcy-Weisbach Formula [37]:

$$P_i^{\text{out}} = P_i^{\text{in}} + \rho g H \tag{1}$$

$$P_{i+1}^{\text{in}} = P_i^{\text{out}} - \rho \cdot g \cdot \frac{0.0246 \cdot \mu^{0.25} \cdot (a_i + b_i \cdot Q_i^{\text{pipe}}) \cdot L_i}{3600^{1.75} \cdot D_i^{4.75}} \cdot rate(C_i^{\text{chem}}) \tag{2}$$

we can control the pumping head, flow rate and drag reduction rate, to achieve IM in STS-RRs, managing the electric pump schedule, multi-batch flow schedule and CDR injection plan in an

integrated manner. However, the pipeline pressure drop estimation error in day-ahead is inevitable, due to factors such as the day-ahead CDR injection plan and the changing ambient environment, which correspond to DDU and DIU in pressure drop in intra-day. They can cause operational insecurity. Hence, we propose a two-stage RIM framework for the processor, which is conceptually consistent with practical STS-RR operations.

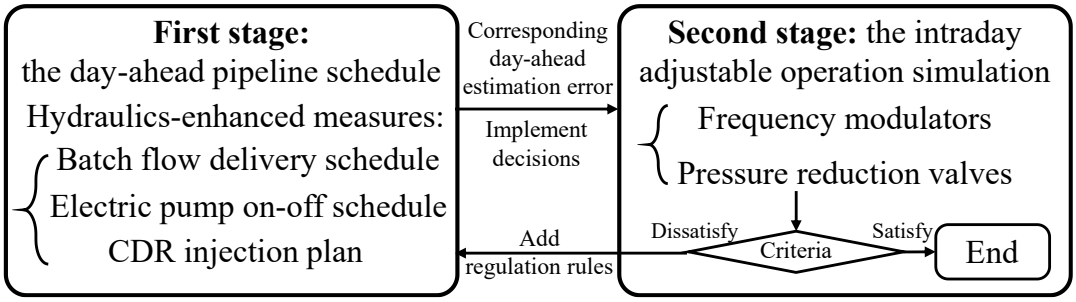

Fig. 2. The proposed two-stage RIM framework.

As illustrated in Fig. 2, in the day-ahead pipeline schedule, the batch flow delivery to be determined beforehand is first obtained. Then, in the intraday adjustable operation simulation, the pipeline schedule is virtually conducted, while the adjustable in-station facilities, such as frequency modulators, should compensate for any possible day-ahead estimation error. If not, regulation rules are added to the first stage and another day-ahead schedule is found. In particular, new formulation for regulation rules are being introduced, as the existing ones for DIU are inadequate for DDU, due to the variability of uncertainty sets with each iteration (as illustrated in Fig. 3). The process lasts until a certain schedule guarantees that the system runs safely and economically. Accordingly, the system operator can coordinate integrated-energy of electricity, LEPs and CDR in the system utilizing hydraulic facilities, to meet the demands of stations with the lowest operation cost, while ensuring secure system operation, which is the scope of RIM in STS-RRs.

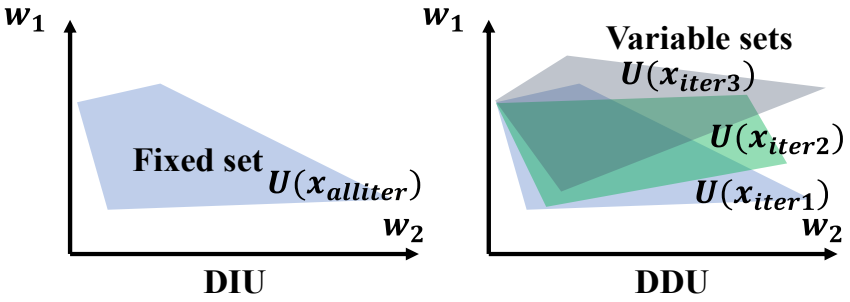

Fig. 3. Conceptual comparison of iterative evolution processes for solving the model under DIU and DDU.

3. Mathematical Formulation

In this section, we introduce the RIM model considering DDU in pressure drop within STS-RRs. The formulation of the day-ahead pipeline schedule, the uncertainty sets and the intraday adjustable operation simulation are given in detail. It is assumed that the LEPs are incompressible and the length of the interface connecting two adjacent batches is neglected [32]. Moreover, as one of the drawbacks, the CDRs are expected to lose their effectiveness when they pass through a station due to the shear force [25]. Consequently, we only consider their influence on the pipeline they are currently in.

3.1. Day-Ahead Pipeline Schedule

The day-ahead pipeline schedule model involves the determination of the electric pump on-off schedule, multi-batch flow schedule and CDR injection plan.

Constraint (3) limits the range of CDR injection concentration. If there is no CDR injection system in the station, $C^{\text{chem}}_{i,\min/\max}$ equal 0.

$$C^{\text{chem}}_{t,i,\min} \le C^{\text{chem}}_{t,i} \le C^{\text{chem}}_{t,i,\max},\ 1 \le t < t_{\max},\ 1 \le i < i_{\max} \tag{3}$$

As the STS-RRs sequentially deliver different products to meet the demands, it is necessary to model the multi-batch migration process. The initial volumetric position of the batches is defined in Eq.(4). Note that the volumetric coordinate of IS is defined as 0, and we imagine a “virtual pipeline”

filled with batches to be uploaded to keep a record of the batch position. The relationship between the forward and backward-end position ($V_{t,b}^{\text{forward}}$ and $V_{t,b}^{\text{backward}}$) of the batches is formulated in Eqns.(5)-(6). Specially, for the last batch $b_{\max}$, its volume change with time is evaluated with $Q_{t,i,b}^{\text{down}}$ and used to determine the position of its backward-end, which is presented in Eq.(7). Constraints Eqns.(8)-(10) indicate the relative volumetric position of the batch forward-end and the stations with time by introducing the variable $B_{t,i,b}^{\text{exc}}$. Constraints (11) and (12) restrict the flow direction and batch sequence, respectively.

$$V_{1,b}^{\text{forward}} = V_{i_{\max}}^{\text{s}} - \sum_{b'=1}^{b-1} V_{b'}^{\text{total}} \tag{4}$$

$$V_{t,b}^{\text{backward}} = V_{t,b+1}^{\text{forward}},\ 1 \le b < b_{\max} \tag{5}$$

$$V_{1,b_{\max}}^{\text{backward}} = V_{1,b_{\max}}^{\text{forward}} - V_{b_{\max}}^{\text{total}} \tag{6}$$

$$V_{t,b_{\max}}^{\text{backward}} = V_{t,b_{\max}}^{\text{forward}} - V_{b_{\max}}^{\text{total}} + \sum_{i=1}^{i_{\max}} \sum_{\tau=1}^{t-1} Q_{\tau,i,b_{\max}}^{\text{down}} \cdot T_t,\ 1 < t < t_{\max} \tag{7}$$

$$V_{t,b}^{\text{forward}} - V_i^{\text{s}} \le B_{t,i,b}^{\text{exc}} \cdot M \tag{8}$$

$$V_{t,b}^{\text{forward}} - V_i^{\text{s}} \ge \left(B_{t,i,b}^{\text{exc}} - 1\right) \cdot M \tag{9}$$

$$V_{t+1,b}^{\text{forward}} - V_i^{\text{s}} \le \left(1 - B_{t+1,i,b}^{\text{exc}} + B_{t,i,b}^{\text{exc}}\right) \cdot M,\ 1 \le t < t_{\max} \tag{10}$$

$$B_{t,i,b}^{\text{exc}} \ge B_{t,i+1,b}^{\text{exc}},\ 1 \le i < i_{\max} \tag{11}$$

$$B_{t,i,b}^{\text{exc}} \ge B_{t,i,b+1}^{\text{exc}},\ 1 \le b < b_{\max} \tag{12}$$

To examine the multi-batch migration process, the change of $V_{t,b}^{\text{forward}}$ should be tracked. Since the forward-end of a single batch can only exist in a pipeline at a time, the variable $B_{t,i,b}^{\text{inpipe}}$ is put forward to distinguish the exact pipeline, which is defined and regulated in Eqns.(13) and (14), respectively. Once a batch is uploaded from IS, the $V_{t,b}^{\text{forward}}$ is updated with the flow rate $Q_{t,i}^{\text{pipe}}$ in the pipeline, given in Eqns.(15) and (16).

$$B_{t,i,b}^{\text{inpipe}} = B_{t,i,b}^{\text{exc}} - B_{t,i+1,b}^{\text{exc}},\ 1 \le i < i_{\max} \tag{13}$$

$$\sum_{b=1}^{b_{\max}} B_{t,i,b}^{\text{inpipe}} \le 1,\ 1 \le i < i_{\max} \tag{14}$$

$$V_{t+1,b}^{\text{forward}} \le V_{t,b}^{\text{forward}} + Q_{t,i}^{\text{pipe}} \cdot T_t + \left(1 - B_{t,i,b}^{\text{inpipe}}\right) \cdot M,\ 1 \le t < t_{\max},\ 1 \le i < i_{\max} \tag{15}$$

$$V_{t+1,b}^{\text{forward}} \ge V_{t,b}^{\text{forward}} + Q_{t,i}^{\text{pipe}} \cdot T_t + \left(B_{t,i,b}^{\text{inpipe}} - 1\right) \cdot M,\ 1 \le t < t_{\max},\ 1 \le i < i_{\max} \tag{16}$$

The LSs and TSs receive different LEPs from the delivered batches through pipeline as demanded. Here, $B_{t,i,b}^{\text{bet}}$, as defined in Eqns.(17) and (18), is utilized to represent whether a station is in between a certain batch so that the station is possible to download LEPs from the batch. Constraint (19) guarantees that a station is just related to a single batch in a time-step. Accordingly, the download flow rate $Q_{t,i,b}^{\text{down}}$ of the station is regulated by $B_{t,i,b}^{\text{bet}}$ through Eq.(20). Besides, $Q_{t,i,b}^{\text{down}}$ is required to be limited in a permitted range in Eq.(21), according to the system design. In Eqns.(22) and (23), for each station, the total downloaded volume should satisfy the evaluated demand for each product, with an allowed deviation margin of $\pm\mu$. The relationship among pipeline flow rates and download flow rates is described in Eq.(24). Constraint (25) shows the secure region of $Q_{t,i}^{\text{pipe}}$

.

$$B_{t,i,b}^{\text{bet}} = B_{t,i,b}^{\text{exc}} - B_{t,i,b+1}^{\text{exc}},\ 1 \le b < b_{\max} \tag{17}$$

$$B_{t,i,b_{\max}}^{\text{bet}} = B_{t,i,b_{\max}}^{\text{exc}} \tag{18}$$

$$\sum_{b=1}^{b_{\max}} B_{t,i,b}^{\text{bet}} = 1 \tag{19}$$

$$Q_{t,i,b}^{\text{down}} \le B_{t,i,b}^{\text{bet}} \cdot M,\ 1 \le t < t_{\max} \tag{20}$$

$$B_{t,i}^{\text{down}} \cdot Q_{i,\min}^{\text{down}} \le \sum_{b=1}^{b_{\max}} Q_{t,i,b}^{\text{down}} \le B_{t,i}^{\text{down}} \cdot Q_{i,\max}^{\text{down}},\ 1 \le t < t_{\max} \tag{21}$$

$$\sum_{t=1}^{t_{\max}-1} \sum_{b=1}^{b_{\max}} o_{b,l} \cdot Q_{t,i,b}^{\text{down}} \cdot T_t \le \left(1+\mu\right) \cdot V_{i,l}^{\text{down}} \tag{22}$$

$$\sum_{t=1}^{t_{\max}-1} \sum_{b=1}^{b_{\max}} o_{b,l} \cdot Q_{t,i,b}^{\text{down}} \cdot T_t \ge \left(1-\mu\right) \cdot V_{i,l}^{\text{down}} \tag{23}$$

$$Q_{t,i}^{\text{pipe}} = Q_{t,i-1}^{\text{pipe}} - \sum_{b=1}^{b_{\max}} Q_{t,i,b}^{\text{down}},\ 1 \le t < t_{\max},\ 1 < i < i_{\max} \tag{24}$$

$$Q_{i,\min}^{\text{pipe}} < Q_{t,i}^{\text{pipe}} < Q_{i,\max}^{\text{pipe}},\ 1 \le t < t_{\max},\ 1 \le i < i_{\max} \tag{25}$$

In the transmission process of LEPs, the fluid overcomes the friction from the pipeline wall as well as the gravity caused by the pipelines' elevation, resulting in pressure drop along the pipeline. Correspondingly, the transmission pumps convert the electric energy to kinetic energy, as compensation for the dynamic pressure against pressure drop. Hence, the pressure drop determines the pumps' pressure output. Note that different products have different physical parameters and thus, their pressure drop incurred are disparate. Furthermore, a single batch can be distributed across two separate pipelines. $P_{t,i}^{\text{drop}}$ is calculated by Eq.(26) derived from Darcy-Weisbach Formula. As frequently switching the pumps on and off may cause damage to them, $B_{t,k_i}^{\text{switch}}$ is used to indicate when the pump state switches (Eqns.(27) and (28)).

$$\begin{aligned}
&P_{t,i}^{\text{drop}} \geq \frac{(\rho_b+\rho_{b+1})/2\cdot g\cdot 0.0246\cdot((\mu_b+\mu_{b+1})/2)^{0.25}}{10^6\cdot 3600^{1.75}\cdot D_i^{4.75}/((a_i+b_i\cdot Q_{t,i}^{\text{pipe}})\cdot L_i)} \\
&+(\rho_{b-1}\cdot g\cdot E_{i+1}-\rho_b\cdot g\cdot E_i)/10^6-(1-B_{t,i,b}^{\text{inpipe}})\cdot M \\
&P_{t,i}^{\text{drop}} \leq \frac{(\rho_b+\rho_{b+1})/2\cdot g\cdot 0.0246\cdot((\mu_b+\mu_{b+1})/2)^{0.25}}{10^6\cdot 3600^{1.75}\cdot D_i^{4.75}/((a_i+b_i\cdot Q_{t,i}^{\text{pipe}})\cdot L_i)} \\
&+(\rho_{b-1}\cdot g\cdot E_{i+1}-\rho_b\cdot g\cdot E_i)/10^6+(1-B_{t,i,b}^{\text{inpipe}})\cdot M, b\in \text{B},\ 1\leq t<t_{\max},\ 1\leq i<i_{\max}
\end{aligned} \tag{26}$$

$$B_{t,k_i}^{\text{switch}} \geq B_{t,k_i}^{\text{pump}} - B_{t-1,k_i}^{\text{pump}},\ 1\leq t<t_{\max},\ 1\leq i<i_{\max} \tag{27}$$

$$B_{t,k_i}^{\text{switch}} \geq B_{t-1,k_i}^{\text{pump}} - B_{t,k_i}^{\text{pump}},\ 1\leq t<t_{\max},\ 1\leq i<i_{\max} \tag{28}$$

Overall, the model for the day-ahead pipeline schedule is summarized in Eq.(29). The objective of this model is to minimize the total cost, which includes both the CDR consumption cost and the labor cost of operating the pumps, over the scheduling horizon.

$$\begin{aligned}
&\min f^{\text{ahead}} = \min \sum_{t=1}^{t_{\max}-1}\sum_{i=1}^{i_{\max}-1}\left(\begin{array}{c}\dfrac{price^{\text{chem}}\cdot\rho^{\text{chem}}\cdot C_{t,i}^{\text{chem}}\cdot Q_i^{\text{pipe}}\cdot T_t}{10^6} \\ +\sum_{k_i\in \text{K}_i} price^{\text{pump}}\cdot B_{t,k_i}^{\text{switch}}\end{array}\right) \\
&\text{s.t. } (1)-(28)
\end{aligned} \tag{29}$$

3.2. DDU and DIU Sets

In the day-ahead pipeline schedule, the nominal pressure drop $P_{t,i}^{\text{drop}}$ is obtained from the

estimation derived using the empirical formula. However, this estimation is subject to uncertainty due to variations in pipeline conditions, and the corresponding pressure drop estimation error $\Delta P_{t,i}^{\mathrm{err}}$ is non-negligible, with its formulation proposed in Eq.(30):

$$\begin{aligned}\Delta P_{t,i}^{\mathrm{err}} \in DDU\left(C_{t,i}^{\mathrm{chem}}, Q_{t,i}^{\mathrm{pipe}}\right) &= \left\{\begin{array}{c}\Delta P_{t,i}^{\mathrm{err}}: \left(C_{t,i}^{\mathrm{chem}}, Q_{t,i}^{\mathrm{pipe}}, \Delta P_{t,i}^{\mathrm{err}}\right) \in \mathrm{conv}\left(\mathrm{V}_i\right),\ i \in \mathrm{I}^{\mathrm{chem}} \\ \mathrm{V}_i = \left\{\left(C_{i,m}^{\mathrm{chem}}, Q_{i,m}^{\mathrm{pipe}}, \Delta P_{i,m}^{\mathrm{err}}\right)\right\}\Big|_{m=1}^{M_i^{\mathrm{DDU}}}\end{array}\right\} \\ &= \left\{\begin{array}{c}\underline{\Delta P_{t,i}^{\mathrm{err}}} \le \Delta P_{t,i}^{\mathrm{err}} \le \overline{\Delta P_{t,i}^{\mathrm{err}}} \\ \underline{\Delta P_{t,i}^{\mathrm{err}}} = \min\limits_{n \in \mathrm{N}_i}\left\{a_{i,n}^{\mathrm{err}} \cdot C_{t,i}^{\mathrm{chem}} + b_{i,n}^{\mathrm{err}} \cdot Q_{t,i}^{\mathrm{pipe}} + c_{i,n}^{\mathrm{err}}\right\},\ \overline{\Delta P_{t,i}^{\mathrm{err}}} = \max\limits_{n \in \mathrm{N}_i}\left\{a_{i,n}^{\mathrm{err}} \cdot C_{t,i}^{\mathrm{chem}} + b_{i,n}^{\mathrm{err}} \cdot Q_{t,i}^{\mathrm{pipe}} + c_{i,n}^{\mathrm{err}}\right\}\end{array}\right\}\end{aligned} \tag{30}$$

where $\mathrm{I}^{\mathrm{chem}}$ is the set of stations with CDR injection systems, $a_{i,n}^{\mathrm{err}}, b_{i,n}^{\mathrm{err}}, c_{i,n}^{\mathrm{err}}$ are calibrated parameters, and $C_{t,i}^{\mathrm{chem}}$, $Q_{t,i}^{\mathrm{pipe}}$ are the day-ahead decisions. The parameters are calibrated offline using industrial supervisory control and data acquisition system data. Specifically, historical records are mapped into a three-dimensional data cloud in the joint space of $\left(C_{t,i}^{\mathrm{chem}}, Q_{t,i}^{\mathrm{pipe}}, \Delta P_{t,i}^{\mathrm{err}}\right)$. Following the idea of data-adaptive convex polyhedral construction in [38], a finite set V_i of M_i^{DDU} support vertices $\left(C_{i,m}^{\mathrm{chem}}, Q_{i,m}^{\mathrm{pipe}}, \Delta P_{i,m}^{\mathrm{err}}\right)\Big|_{m=1}^{M_i^{\mathrm{DDU}}}$ is derived from the data cloud, and then a polytope in the joint space is constructed as the convex hull of V_i. This polytope serves as a tractable geometric surrogate that captures the empirical dependence structure among $\left(C_{t,i}^{\mathrm{chem}}, Q_{t,i}^{\mathrm{pipe}}, \Delta P_{t,i}^{\mathrm{err}}\right)$. Importantly, Eq.(30) provides an equivalent interval representation of the intersection line $\mathrm{conv}\left(\mathrm{V}_i\right)\Big|_{C_{t,i}^{\mathrm{chem}}, Q_{t,i}^{\mathrm{pipe}}}$ (i.e., $\underline{\Delta P_{t,i}^{\mathrm{err}}} \le \Delta P_{t,i}^{\mathrm{err}} \le \overline{\Delta P_{t,i}^{\mathrm{err}}}$) of the polytope, at the day-ahead decisions $C_{t,i}^{\mathrm{chem}}$ and $Q_{t,i}^{\mathrm{pipe}}$. Therefore, the parameters correspond to coefficients of the facet-defining inequalities of the calibrated polytope and can be treated as pipeline-specific constants over a one-day scheduling horizon. The induced uncertainty set for $\Delta P_{t,i}^{\mathrm{err}}$ varies with $C_{t,i}^{\mathrm{chem}}$ and $Q_{t,i}^{\mathrm{pipe}}$,which is the defining characteristic of DDU. The formulation of DIU sets is given in Eq.(31), where $\Delta P_{t,i,\min/\max}^{\mathrm{err}}$ are also derived from the on-site data.

$$\Delta P_{t,i}^{\mathrm{err}} \in DIU = \left\{\begin{array}{c}\Delta P_{t,i,\min}^{\mathrm{err}} \le \Delta P_{t,i}^{\mathrm{err}} \le \Delta P_{t,i,\max}^{\mathrm{err}} \\ i \in \mathrm{I} - \mathrm{I}^{\mathrm{chem}}\end{array}\right\} \tag{31}$$

3.3. Intraday Adjustable Operation Simulation

In the intraday, the STS-RR operates the adjustable in-station facilities corresponding to the estimation errors within the uncertainty set. This process is simulated by the processor in the second stage of the proposed framework. Note that the decisions from the day-ahead stage are considered as parameters in the intraday stage. Detailed model descriptions are as follows.

The max-min problem of the intraday adjustable operation simulation in Eq.(32) is to evaluate the electricity cost in the worst-case scenario. The pressure distribution and energy balance along the pipeline system is described in Eqns.(33)-(35). Constraints (36) and (37) set the security region for the inlet and outlet pressure of each station. In Eqns.(38)-(40), the pressure provided by a station is the total actual output P_{t,k_i}^{actu} of the in-station pumps, which is regulated by B_{t,k_i}^{pump} and P_{t,k_i}^{head}. Constraints (41) explains that P_{t,k_i}^{head} follows the Pascal's law of the fluid pressure. The base-frequency pumping head H_{t,k_i}^{base} of the pumps is calculated by Eq.(42). On the industrial site, frequency modulators are equipped for flexible pump output. Consequently, the modulated pumping head can be adjusted within the permissible range defined by H_{t,k_i}^{base}. Constraints (44) and (45) demonstrate the total electric energy consumed by a station and a transmission pump, respectively.

$$\Gamma^{\text{intra}} = \max_{\Delta P_{t,i}^{\text{err}} \in U} \min_{W_{t,i}^{\text{station}}} f^{\text{intra}} = \max_{\Delta P_{t,i}^{\text{err}} \in U} \min_{W_{t,i}^{\text{station}}} \sum_{t=1}^{t_{\max}-1} \sum_{i=1}^{i_{\max}-1} price_{t,i}^{\text{ele}} \cdot W_{t,i}^{\text{station}} \cdot 10^3 \tag{32}$$

s.t.

$$P_{t,i}^{\text{out}} = P_{t,i}^{\text{in}} + P_{t,i}^{\text{station}},\ 1 \le t < t_{\max},\ 1 \le i < i_{\max} \tag{33}$$

$$P_{t,i+1}^{\text{in}} = P_{t,i}^{\text{out}} - P_{t,i}^{\text{drop}} + \Delta P_{t,i}^{\text{err}},\ 1 \le t < t_{\max},\ 1 \le i < i_{\max} \tag{34}$$

$$P_{t,1}^{\text{in}} = P^{\text{feed}},\ 1 \le t < t_{\max} \tag{35}$$

$$P_{i,\min}^{\text{in}} \le P_{t,i}^{\text{in}} \le P_{i,\max}^{\text{in}},\ 1 \le t < t_{\max},\ 1 < i < i_{\max} \tag{36}$$

$$P_{i,\min}^{\text{out}} \le P_{t,i}^{\text{out}} \le P_{i,\max}^{\text{out}},\ 1 \le t < t_{\max},\ 1 \le i < i_{\max} \tag{37}$$

$$P_{t,i}^{\text{station}} = \sum_{k_i \in \mathrm{K}_i} P_{t,k_i}^{\text{actu}},\ 1 \le t < t_{\max},\ 1 \le i < i_{\max} \tag{38}$$

$$-\left(1 - B_{t,k_i}^{\text{pump}}\right) \cdot M + P_{t,k_i}^{\text{head}} \le P_{t,k_i}^{\text{actu}} \le \left(1 - B_{t,k_i}^{\text{pump}}\right) \cdot M + P_{t,k_i}^{\text{head}},\ 1 \le t < t_{\max},\ 1 \le i < i_{\max} \tag{39}$$

$$-B_{t,k_i}^{\text{pump}} \cdot M \le P_{t,k_i}^{\text{actu}} \le B_{t,k_i}^{\text{pump}} \cdot M,\ 1 \le t < t_{\max},\ 1 \le i < i_{\max} \tag{40}$$

$$P_{t,k_i}^{\text{head}} = \rho_i \cdot g \cdot H_{t,k_i}^{\text{mod}} / 10^6,\ 1 \le t < t_{\max},\ 1 \le i < i_{\max} \tag{41}$$

$$\begin{aligned} H_{t,k_i}^{\text{base}} &= a_{k_i}^{\text{pump}} \cdot \left(Q_i^{\text{pipe}}\right)^2 + b_{k_i}^{\text{pump}} \cdot Q_i^{\text{pipe}} + c_{k_i}^{\text{pump}} \\ &+ \left(2 \cdot a_{k_i}^{\text{pump}} \cdot Q_i^{\text{pipe}} + b_{k_i}^{\text{pump}} \cdot Q_i^{\text{pipe}}\right) \cdot \left(Q_{t,i}^{\text{pipe}} - Q_i^{\text{pipe}}\right),\ 1 \le t < t_{\max},\ 1 \le i < i_{\max} \end{aligned} \tag{42}$$

$$\kappa \cdot H_{t,k_i}^{\text{base}} \le H_{t,k_i}^{\text{mod}} \le H_{t,k_i}^{\text{base}},\ 1 \le t < t_{\max},\ 1 \le i < i_{\max} \tag{43}$$

$$W_{t,i}^{\text{station}} = \sum_{k_i \in \mathrm{K}_i} W_{t,k_i}^{\text{actu}},\ 1 \le t < t_{\max},\ 1 \le i < i_{\max} \tag{44}$$

$$W_{t,k_i}^{\text{actu}} = P_{t,k_i}^{\text{actu}} \cdot Q_i^{\text{pipe}} \cdot T_t / 3600,\ 1 \le t < t_{\max},\ 1 \le i < i_{\max} \tag{45}$$

3.4. Robust Compact Form

For the convenience of introducing the solution methodology in the next section, the proposed RIM model considering DDU in STS-RRs is written in its robust compact form in Eq.(46), where $\boldsymbol{x}$ and $\boldsymbol{y}$ are the vectors consisting of decision variables associated with the first and second stage, respectively, $\boldsymbol{\omega}$ is the vector of $\{\Delta P_{t,i}^{\text{err}}\}$, and the other vectors as well as matrices are coefficients of variable vectors or constant terms in objective function $f^{\text{intra}}(\boldsymbol{y})$ and inequalities. Note that the equations are transformed into their respective inequality forms.

$$\begin{aligned} &\min_{\boldsymbol{x} \in X} f^{\text{ahead}}(\boldsymbol{x}) + \Gamma^{\text{intra}}(\boldsymbol{x}) = \min_{\boldsymbol{x} \in X} f^{\text{ahead}}(\boldsymbol{x}) + \max_{\boldsymbol{\omega} \in U(\boldsymbol{x})} \min_{\boldsymbol{y} \in Y(\boldsymbol{x}, \boldsymbol{\omega})} f^{\text{intra}}(\boldsymbol{y}) = \min_{\boldsymbol{x} \in X} f^{\text{ahead}}(\boldsymbol{x}) + \max_{\boldsymbol{\omega} \in U(\boldsymbol{x})} \min_{\boldsymbol{y} \in Y(\boldsymbol{x}, \boldsymbol{\omega})} \boldsymbol{c}^{\mathrm{T}} \boldsymbol{y} \\ &\text{s.t.} \quad X = \{(1) - (28)\} \\ &U(\boldsymbol{x}) = \{\boldsymbol{G}\boldsymbol{\omega} \le \boldsymbol{h} + \boldsymbol{H}\boldsymbol{x}\} = \{(30) - (31)\} \\ &Y(\boldsymbol{x}, \boldsymbol{\omega}) = \{\boldsymbol{A}\boldsymbol{x} + \boldsymbol{B}\boldsymbol{y} + \boldsymbol{C}\boldsymbol{\omega} \le \boldsymbol{d}\} = \{(33) - (45)\} \end{aligned} \tag{46}$$

4. Solution Methodology

To examine whether the system runs safely and economically under the day-ahead pipeline schedule, specific criteria are to be designed for the intraday adjustable operation simulation. Correspondingly, regulation rules should be incorporated into the first stage to facilitate its understanding of the second stage. In this paper, the idea of parametric C&CG algorithm [28] is

applied to propose the workflow of the two-stage RIM framework with the established model.

The detailed workflow is shown in TABLE II, where five steps are included. Specifically, the processor first gathers the input information and then initializes the sets parameters. In the day-ahead pipeline schedule, a non-negative variable η is introduced as the auxiliary variable to estimate $\Gamma^{\text{intra}}(\boldsymbol{x})$ (by solving MP) in the first stage. The first criterion is to judge whether the STS-RR is capable of meeting the demands. Subsequently, the intraday adjustable operation simulation is conducted. The feasibility of $\boldsymbol{x}^*$ derived from the first stage is examined by solving SP1. Note that all the bilevel optimization problems in this paper are transformed into a tractable formulation by dualizing the inner-level problem and employing the KKT conditions. If $\boldsymbol{x}^*$ is feasible, the economic examination of $\boldsymbol{x}^*$ is done and the economic regulation rule is added to the MP, otherwise security regulation rule is obtained and incorporated into the MP. Eventually, the second criterion distinguishes whether the processor finds the day-ahead pipeline schedule to achieve safe and economical STS-RR operation. If it is the case, the day-ahead pipeline schedule is output for execution in real time.

Step1. Gather the locally evaluated product demands, operation data and the system design parameters.

Step2. Initialize $LB = 0$, $UB = \inf$, $iter = 1$, $\text{Constraints1} = \text{Constraints2} = \varnothing$ and $\text{Constraints} = \{\boldsymbol{x} \in X,\ \eta \geq 0\}$.

Step3. Do the **Day-ahead pipeline schedule (first stage)**:

MP: $\min f^{\text{ahead}}(\boldsymbol{x}) + \eta$
s.t. Constraints

Derive $\boldsymbol{x}^*$, η^* and set $LB = f^{\text{ahead}}(\boldsymbol{x}^*) + \eta^*$.

Criterion 1: If MP is infeasible, the demands of STS-RRs cannot be fulfilled. The system operate should rearrange the demands and go to **Step1**.

Step4. Indentify the worst-case scenario in the **intraday adjustable operation simulation (second stage)**:

(1) Examine the feasiability of $\boldsymbol{x}^*$ by solving the SP1:

SP1: $\Gamma_1^{\text{intra}}\left(\boldsymbol{x}^*\right)=\max\limits_{\boldsymbol{\omega}}\min\limits_{\boldsymbol{y},\boldsymbol{y}_s}1^{\mathrm{T}}\boldsymbol{y}_s$

s.t. $\boldsymbol{\omega}\in U\left(\boldsymbol{x}^*\right):\boldsymbol{\xi},\ \boldsymbol{A}\boldsymbol{x}^*+\boldsymbol{B}\boldsymbol{y}+\boldsymbol{C}\boldsymbol{\omega}\le\boldsymbol{d}+\boldsymbol{y}_s:\boldsymbol{\zeta},\ \boldsymbol{y}_s\ge 0$

$\overset{\text{dualize, KKT}}{\Rightarrow}\ \Gamma_1^{\text{intra}}\left(\boldsymbol{x}^*\right)=\max\limits_{\boldsymbol{\omega},\boldsymbol{\xi},\boldsymbol{\zeta}}\boldsymbol{\zeta}^{\mathrm{T}}\left(\boldsymbol{A}\boldsymbol{x}^*-\boldsymbol{d}\right)-\boldsymbol{\xi}^{\mathrm{T}}\left(\boldsymbol{h}+\boldsymbol{H}\boldsymbol{x}^*\right)$

s.t. $0\le\boldsymbol{\zeta}\le 1,\ \boldsymbol{B}^{\mathrm{T}}\boldsymbol{\zeta}\ge 0,\ \boldsymbol{C}^{\mathrm{T}}\boldsymbol{\zeta}+\boldsymbol{G}^{\mathrm{T}}\boldsymbol{\xi}=0$

$-z_1\cdot M\le\boldsymbol{\xi}\le 0,\ z_1\in\{0,1\},\ -\left(1-z_1\right)\cdot M\le\boldsymbol{G}\boldsymbol{\omega}-\boldsymbol{h}-\boldsymbol{H}\boldsymbol{x}^*\le 0$

Derive $\boldsymbol{\omega}^*$ and $\Gamma_1^{\text{intra}}\left(\boldsymbol{x}^*\right)$.

(2) If $\Gamma_1^{\text{intra}}\left(\boldsymbol{x}^*\right)=0$, i.e., $\boldsymbol{x}^*$ is feasible, obtain the economic regulation rule by solving the SP2:

SP2: $\Gamma_2^{\text{intra}}\left(\boldsymbol{x}^*\right)=\max\limits_{\boldsymbol{\omega}}\min\limits_{\boldsymbol{y}}\boldsymbol{c}^{\mathrm{T}}\boldsymbol{y}$

s.t. $\boldsymbol{\omega}\in U\left(\boldsymbol{x}^*\right):\boldsymbol{\theta},\ \boldsymbol{y}\in Y\left(\boldsymbol{x}^*,\boldsymbol{\omega}\right):\boldsymbol{\varsigma}$

$\overset{\text{dualize, KKT}}{\Rightarrow}\ \Gamma_2^{\text{intra}}\left(\boldsymbol{x}^*\right)=\max\limits_{\boldsymbol{\omega},\boldsymbol{\theta},\boldsymbol{\varsigma}}\boldsymbol{\varsigma}^{\mathrm{T}}\left(\boldsymbol{A}\boldsymbol{x}^*-\boldsymbol{d}\right)-\boldsymbol{\theta}^{\mathrm{T}}\left(\boldsymbol{h}+\boldsymbol{H}\boldsymbol{x}^*\right)$

s.t. $\boldsymbol{\varsigma}\ge 0,\ \boldsymbol{B}^{\mathrm{T}}\boldsymbol{\varsigma}+\boldsymbol{c}\ge 0,\ \boldsymbol{C}^{\mathrm{T}}\boldsymbol{\varsigma}+\boldsymbol{G}^{\mathrm{T}}\boldsymbol{\theta}=0$

$-z_2\cdot M\le\boldsymbol{\theta}\le 0,\ z_2\in\{0,1\},\ -\left(1-z_2\right)\cdot M\le\boldsymbol{G}\boldsymbol{\omega}-\boldsymbol{h}-\boldsymbol{H}\boldsymbol{x}^*\le 0$

Derive $\boldsymbol{\varsigma}^*$ and set $UB=\min\left\{UB,f^{\text{ahead}}\left(\boldsymbol{x}^*\right)+\Gamma_2^{\text{intra}}\left(\boldsymbol{x}^*\right)\right\}$.

Regulation rule 1: Economic regulation rule

Constraints1=$\{\eta\ge\boldsymbol{c}^{\mathrm{T}}\boldsymbol{y}_{\boldsymbol{\varsigma}^*}$

$\boldsymbol{A}\boldsymbol{x}+\boldsymbol{B}\boldsymbol{y}_{\boldsymbol{\varsigma}^*}+\boldsymbol{C}\boldsymbol{\omega}_{\boldsymbol{\varsigma}^*}\le\boldsymbol{d},\ \boldsymbol{C}^{\mathrm{T}}\boldsymbol{\varsigma}^*+\boldsymbol{G}^{\mathrm{T}}\boldsymbol{\theta}_{\boldsymbol{\varsigma}^*}=0,\ z_{\boldsymbol{\varsigma}^*}\in\{0,1\}$

$-z_{\boldsymbol{\varsigma}^*}\cdot M\le\boldsymbol{\theta}_{\boldsymbol{\varsigma}^*}\le 0,\ -\left(1-z_{\boldsymbol{\varsigma}^*}\right)\cdot M\le\boldsymbol{G}\boldsymbol{\omega}_{\boldsymbol{\varsigma}^*}-\boldsymbol{h}-\boldsymbol{H}\boldsymbol{x}\le 0\}$

Update Constraints=Constraints$\cup$Constraints1 and Constraints1$=\varnothing$.

(3) If $\Gamma_1^{\text{intra}}\left(\boldsymbol{x}^*\right)>0$, i.e., $\boldsymbol{x}^*$ is infeasible, obtain the security regulation rule by solving SP3:

SP3: $\Gamma_3^{\text{intra}}\left(\boldsymbol{x}^*\right)=\min\limits_{\boldsymbol{y}}\boldsymbol{c}^{\mathrm{T}}\boldsymbol{y}$

s.t. $\boldsymbol{y}\in Y\left(\boldsymbol{x}^*,\boldsymbol{\omega}^*\right):\boldsymbol{\gamma}$

$\overset{\text{dualize}}{\Rightarrow}\ \Gamma_3^{\text{intra}}\left(\boldsymbol{x}^*\right)=\max\limits_{\boldsymbol{\theta},\boldsymbol{\varsigma}}\boldsymbol{\gamma}^{\mathrm{T}}\left(\boldsymbol{A}\boldsymbol{x}^*+\boldsymbol{C}\boldsymbol{\omega}^*-\boldsymbol{d}\right)$ then Derive $\boldsymbol{\gamma}^*$.

s.t. $\boldsymbol{\gamma}\ge 0,\ \boldsymbol{B}^{\mathrm{T}}\boldsymbol{\gamma}+\boldsymbol{c}\ge 0$

Regulation rule 2: Security regulation rule

Constraints2=$\{\boldsymbol{A}\boldsymbol{x}+\boldsymbol{B}\boldsymbol{y}_{\boldsymbol{\gamma}^*}+\boldsymbol{C}\boldsymbol{\omega}_{\boldsymbol{\gamma}^*}\le$ d

$\boldsymbol{C}^{\mathrm{T}}\boldsymbol{\gamma}^*+\boldsymbol{G}^{\mathrm{T}}\boldsymbol{\xi}_{\boldsymbol{\gamma}^*}=0,\ z_{\boldsymbol{\gamma}^*}\in\{0,1\}$

$-z_{\boldsymbol{\gamma}^*}\cdot M\le\boldsymbol{\xi}_{\boldsymbol{\gamma}^*}\le 0,\ -\left(1-z_{\boldsymbol{\gamma}^*}\right)\cdot M\le\boldsymbol{G}\boldsymbol{\omega}_{\boldsymbol{\gamma}^*}-\boldsymbol{h}-\boldsymbol{H}\boldsymbol{x}\le 0\}$

Update Constraints=Constraints$\cup$Constraints2 and Constraints2$=\varnothing$.

Step5. Criterion 2: If $UB-LB\le\varepsilon$, the RIM framework is considered to find the day-ahead pipeline schedule to achieve safe and economical STS-RR operation. Otherwise, set $iter=iter+1$ and go to **Step3**.

TABLE II Workflow of two-stage RIM framework

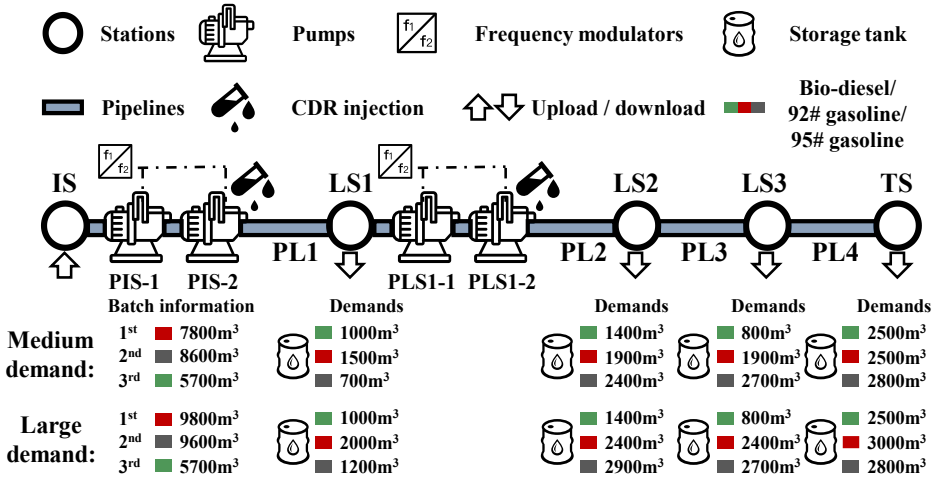

Fig. 4. Configuration of an illustrative 5-bus STS-RR.

5. Case Studies

In this section, case studies on an illustrative 5-bus STS-RR and a real-world cross-regional STS-RR are carried out to verify the safety and economic performances, as well as the scalability of the proposed framework. The configuration of an illustrative 5-bus STS-RR is shown in Fig. 4. The system has 4 pipeline segments and 4 pumps (2 for IS, and 2 for LS1) equipped with frequency modulators. Three types of LEPs, including bio-diesel, 92# gasoline, and 95# gasoline (in China), are aggregated into batches and sequentially transmitted from IS to TS to meet the demands. It is assumed that the system is initially filled with bio-diesel at the beginning of operations. The CDR is injected from IS and LS1 into the respective pipelines. Two scenarios, specifically designed for demonstration purposes, include medium and large local demands. Detailed parameters for the products and the system elements are given in TABLE III-TABLE V. Additionally, the electricity price accords with the real-world electricity market in South China during the high water period, and the CDR price and labor cost are set to 13 (¥/kg) and 100 (¥) according to the operational experience on site, respectively. The uncertainty sets are established based on the data from the industrial supervisory control and data acquisition system and tailored for the illustrative STS-RR. The verification of the proposed framework under the illustrative 5-bus STS-RR is shown as follows.

Products	ρ_l (kg/m^3)	μ_l (m^2/s)
Bio-diesel	847.4	6×10^{-6}
92# gasoline	724	2×10^{-6}
95# gasoline	725	1×10^{-6}

TABLE III Physical properties of LEPs

Pipelines	L_i (km) /	D_i (mm) /	Δh_i (m)	$Q^{\text{pipe}}_{i,\min/\max}$ (m^3/h)
PL1	15.1	355.6	25	500/1200
PL2	12.1	355.6	35	500/1200
PL3	10.1	355.6	80	100/1100
PL4	10.1	355.6	80	100/800

TABLE IV Basic data of pipelines

Stations	$P^{in}_{i,\min/\max}$ (MPa)	$P^{\text{out}}_{i,\min/\max}$ (MPa)	$Q^{\text{down}}_{i,\min/\max}$ (m^3/h)
IS	0.3/0.5	1.2/6.8	0/1200
LS1	0.8/4.9	0.8/5.3	100/900
LS2	0.5/3.8	0.5/3.8	100/900
LS3	0.5/3.0	0.5/3.0	100/800
TS	0.5/3.0	/	100/600

TABLE V Basic Data of Stations

Pumps	$a^{\text{pump}}_{k_i}$ ($\times10^{-6}$ h^2/m^5)	$b^{\text{pump}}_{k_i}$ ($\times10^{-2}$ h/m^2)	$c^{\text{pump}}_{k_i}$ (m)
PIS-1/2	-1.09	-14.1	497.1
PLS1-1/2	-40.49	5.6	322.9

TABLE VI Basic data of pumps

5.1. Necessity of Proposed IM

The following cases representing different STS-RR energy management strategies are designed to investigate the necessity of IM for system operation. Note that all the cases in this subsection ignore the uncertainties to emphasize IM's intrinsic advantage.

Case 1a: the STS-RR executes the proposed IM.

Case 1b: the STS-RR conducts the joint flow delivery and electric pump scheduling, without considering the usage of CDR.

Case 1c: the STS-RR first makes flow delivery schedule and then obtains electric pump scheduling, without considering the usage of CDR.

Comparison terms		**Case 1a**	Case 1b	Case 1c
		Medium demand		
Day-ahead cost (¥)	CDR	**2105.93**	0	0
	Labor	**700**	600	1200
Intraday cost (¥): electricity		**12631.11**	17096.18	18642.31
Total operation cost (¥)		**15437.04**	17696.18	19842.31
Energy efficiency improvement ratio r_{en} (%)		**32.24**	8.29	0 (baseline)
Economic improvement ratio r_{ec} (%)		**22.20**	10.81	0 (baseline)
LEP turnover [32] (10^3 ton·km)		**189.60**	189.60	189.60
		Large demand		
Day-ahead cost (¥)	CDR	**2345.68**	0	0
	Labor	**200**	800	600
Intraday cost (¥): electricity		**16171.70**	17928.44	12256.95
Total operation cost (¥)		**18717.38**	18728.44	12856.95
LEP turnover (10^3 ton·km)		**216.63**	192.80	171.82
Turnover improvement ratio r_t (%)		**26.08**	12.21	0 (baseline)

TABLE VII STS-RR energy management strategy comparisons

The results are summarized in TABLE VII, which includes the performance metrics for the cases under both medium and large local demand scenarios. For medium demand scenario, all the energy management strategies ensure safe system operation, achieving a turnover of 189,600 ton·km. The strategy in Case 1c exhibits the worst economic performance. This is due to the separate flow delivery and pump schedules, which neglects the coordinative effects between the two processes. In comparison, the joint flow delivery and pump scheduling in Case 1b collaboratively considers both transmission turnover and costs, resulting in a total economic improvement of 10.81%. Notably, the proposed IM achieves improvements of 32.24% in total energy consumption and 22.20% in cost. Despite incurring slightly higher CDR and labor expenses compared with other strategies, the use of CDR notably lowers the intraday electricity cost. In addition, the detailed electric pump schedule of three cases is presented in Fig. 5. Comparing Case 1a with Case 1b, fewer pumps are started up due to the effect of CDR. Also comparing Case 1b with Case 1c, the joint

scheduling coordinates the spatial and temporal flow distribution in the pipeline to cooperate with pumps, which leads to fewer pumps' usage and less energy consumption. Therefore, under the same transmission turnover, the proposed IM achieves substantial improvement in total cost and energy efficiency.

As for large local demand, without the CDR usage, Case 1b is forced to reduce its transmission turnover to enable the system security. Comparatively, the proposed IM in Case 1a fully satisfies local demands, achieves an 26.08% improvement in turnover compared to Case 1c, and still demonstrates better economic performance than Case 1b. We further adjust the pressure security region to facilitate the feasibility of Case 1b at the same turnover as Case 1a and, accordingly, a comparison of operation security on PL2 between Case 1a and Case 1b is shown in Fig. 6. In hours 6-7, the inlet pressure of PL2 in (a) is observed to be higher than that in (b). This discrepancy is attributed to the differing flow rates in the pipelines across these two cases at these specific time-steps, which are adjusted actively by IM. For Case 1a, with the help of IM, the pressure distribution along the pipeline always remains within security limits, whereas Case 1b falls into the unsecure region, causing security issues. Additionally, for PL2, the pressure drop reduction ratio averages 31.79%. Overall, the proposed IM is essential for ensuring safe and highly economic STS-RR operation while guaranteeing sufficient demands. The introduction of CDR significantly decreases the pressure drop, reducing the energy required to overcome fluid friction and thereby lowering electricity costs.

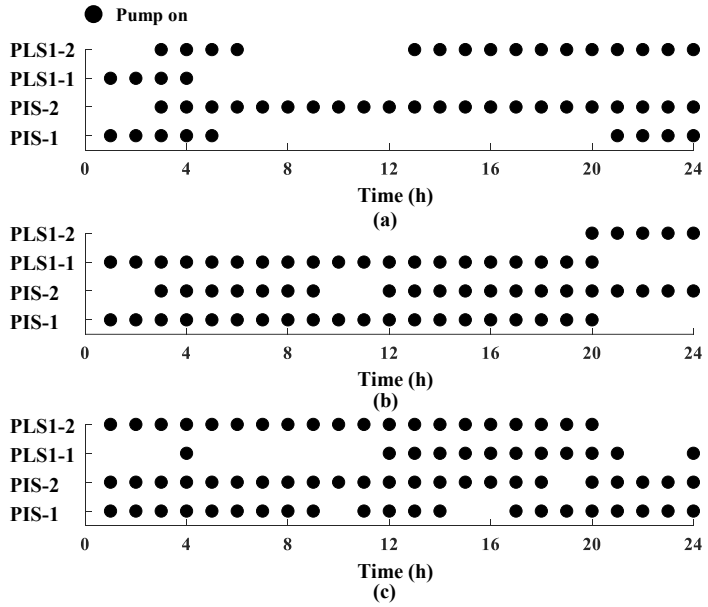

Fig. 5. Electric pump schedule comparison. (a) Case 1a; (b) Case 1b; (c) Case 1c.

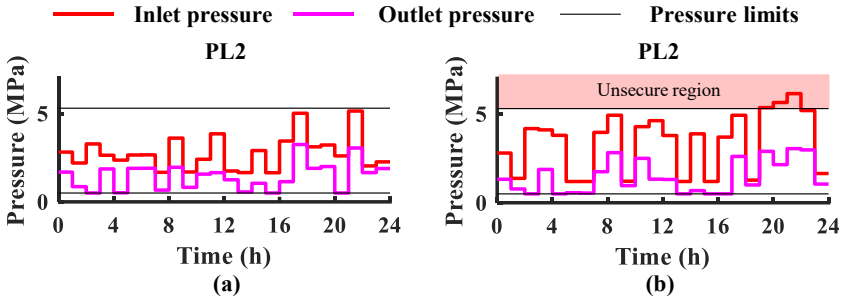

Fig. 6. Pressure distribution in PL2. (a) Case 1a; (b) Case 1b.

5.2. Performance of RIM

Another case is designed as follows based on Case 1a with large demand, to further illustrate the robust performance of the proposed RIM framework.

Case 2: the STS-RR executes the proposed two-stage RIM framework under the large local demand scenario, considering the uncertainties.

5.2.1. RIM Results

In Fig. 7, the detailed day-ahead pipeline schedule for Case 2 is presented. The total operation cost is 21,119.42 ¥, higher than that in Case 1a (18,717.38 ¥), which is attributed to dealing with uncertainties. Within the batch flow delivery schedule, the upload/download flow rates of the stations indicate the pipeline turnover by the width and the system meets the demanded turnover of 216,630 ton·km, consistent with the results in Case 1a. The pump schedule shows the robust on-off

states, where pumps are turned on most of the time for secure operation backup, intuitively compared with Fig. 5 (a). Correspondingly, the CDR injection plan displays the injection concentration over the scheduled horizon in detail.

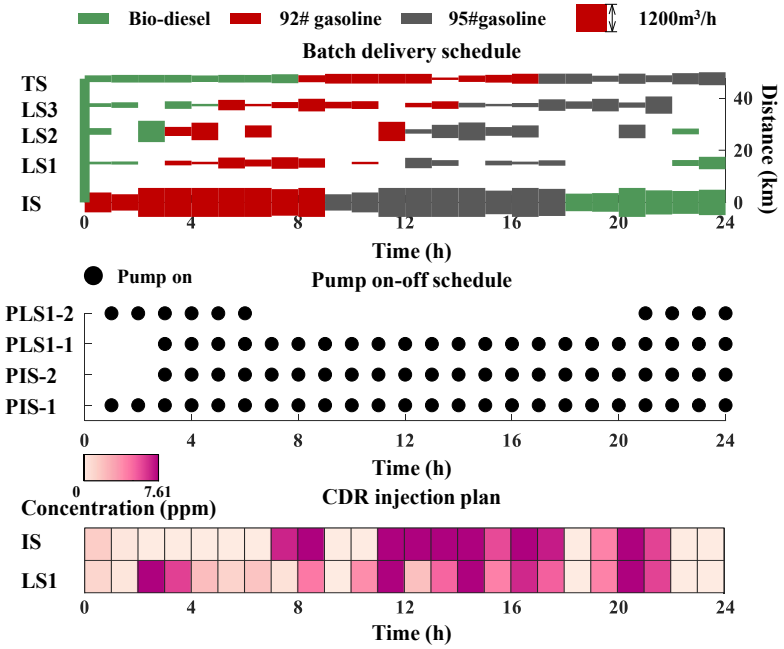

Fig. 7. Day-ahead pipeline schedule in Case 2.

In Fig. 8, the iterative evolution of the proposed workflow is depicted, demonstrating convergence after four iterations. Additionally, the robust infeasibility level indicates that the RIM framework complies with the security regulations following the 2nd iteration. Specifically, the DDU sets of PL1 corresponding to the last iteration over the entire horizon are presented in Fig. 9. The thick lines represent the minimum and maximum random variation range for PL1 with CDR injection, respectively, and the thin lines indicate the extracted extreme scenarios. The variations in pipeline pressure drop within the DDU sets significantly depend on the flow rates and CDR injection concentration in Fig. 7, and these dependencies vary across different time-steps. This highlights the significance of considering DDU in this paper. In addition, the proposed workflow is capable of extracting extreme scenarios and leads the solution to convergence with DDU.

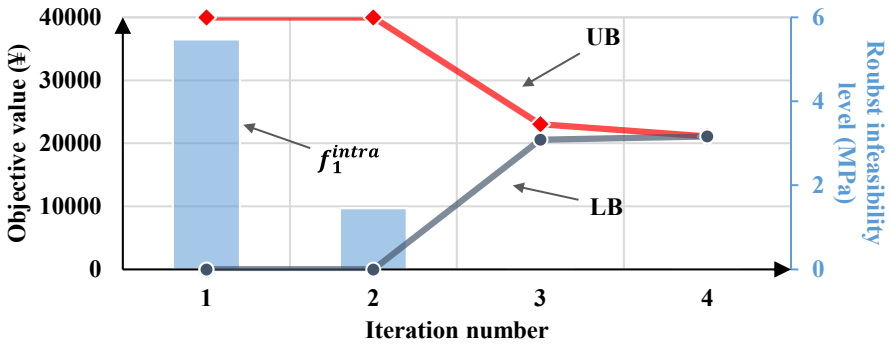

Fig. 8. Evolution of the proposed workflow.

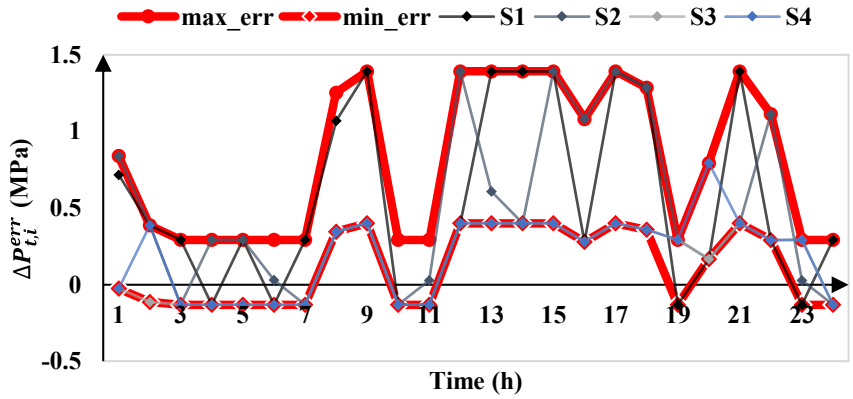

Fig. 9. DDU sets and extreme scenarios of PL1 at different time-steps.

5.2.2. Out-of-Sample Assessment

Out-of-sample assessment is also conducted to evaluate the performance of the proposed model in terms of feasibility and cost [39]. Scenarios are randomly generated from a normal distribution with a mean of $\Delta P_{t,i}^{\text{err}}$ and the standard variance of 0.2, 0.4, 0.6 MPa, respectively. Five hundred scenarios are tested for each setting and the number of infeasible scenarios, the average sampled infeasibility level (ASIL) and the average sampled intraday cost (ASIC) are recorded in TABLE VIII. Note that the ASIL is defined as the average value of the samples' $\Gamma_1^{\text{intra}}\left(\boldsymbol{x}^*\right)$ and ASIC is defined as the average value of $\Gamma_2^{\text{intra}}\left(\boldsymbol{x}^*, \Delta P_{t,i}^{\text{err,sampled}}\right) + \text{accidentcost} \times \text{ASIL}$ over all samples, where the accident cost is set to 10000 (¥/MPa). As the standard variance increases, the number of infeasible scenarios rises in both Case 1a and Case 2. However, Case 1a exhibits significantly more infeasible scenarios than Case 2 across different standard variances. Notably, when the standard variance is 0.6 MPa, which represents a stress-test setting, only 13 scenarios are infeasible in Case

2, resulting in minimal cost increase, whereas Case 1a experiences a substantial cost boost. Consequently, the result in Case 1a struggles to handle uncertain parameters, while that in Case 2 can accommodate a relatively wide range of uncertainty variations.

Overall, the robust pipeline schedule obtained in Case 2 further offers practical guidance for on-site dispatchers to safely operate the system corresponding to uncertain estimation errors, although a slight increase in cost is negligible.

	Standard variance (MPa)	0.2	0.4	0.6
Case 1a	Infeasiable scenarios	434	453	481
	ASIL (MPa)	0.5742	1.3749	2.8370
	ASIC (¥)	24135.50	32198.34	46861.06
Case 2	Infeasiable scenarios	0	1	13
	ASIL (MPa)	0	4.04e-05	0.0582
	ASIC (¥)	18837.29	18846.29	19409.44

TABLE VIII Out-of-sample assessment results

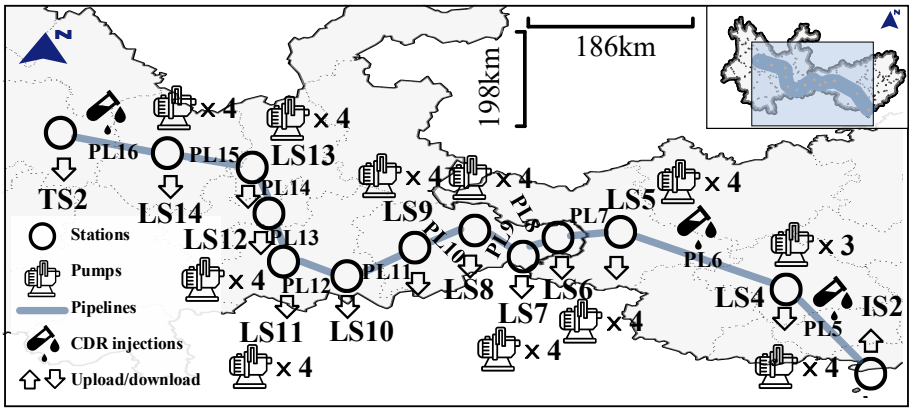

Fig. 10. Configuration of the real-world cross-regional STS-RR in China.

5.2.3. Test with Real-World Cross-Regional STS-RR in China

In this subsection, case studies on the real-world cross-regional STS-RR, which is in detail an industrial multi-product transmission system, over 24 h horizon are applied to further validate the effectiveness and scalability of the RIM framework. The system is configured in Fig. 10. It distributes across three large administrative provinces in South China, which is totally 1,579.33 km long with 12 pipelines and 43 pumps, and meets the refined oil demand within a range of 735,260 km^2, rather large in scale compared with most studied pipelines [31]. Other detailed parameters can

be accessed from the on-line supplementary datasheet [40].

Three more cases are conducted to illustrate the economic efficiency of the proposed framework in handling uncertainties:

Case 3a: the real-world cross-regional STS-RR executes the proposed two-stage RIM framework, considering DDU sets.

Case 3b: the real-world cross-regional STS-RR executes the proposed two-stage RIM framework, but without the economic regulation rule, considering DDU sets.

Case 3c: the real-world cross-regional STS-RR operates with the proposed two-stage RIM framework, but without the CDR injection, considering DDU sets.

Case 3d: the real-world cross-regional STS-RR operates with the proposed two-stage RIM framework, considering only DIU sets.

Comparison terms		**Case 3a**	Case 3b	Case 3c	Case 3d
Day-ahead cost (¥)	CDR	**4694.49**	0	0	0
	Labor	**0**	0	500	700
Intraday cost (¥): electricity		**146955.95**	177456.52	169926.75	171872.72
Total cost (¥)		**151650.44**	177456.52	170426.75	172572.72
Economic improvement ratio r_{ec} (%)		**12.12**	-2.83	1.25	0 (baseline)
LEP turnover (10^3 ton·km)		**3702.83**	3702.83	3702.83	3702.83

TABLE IX Economic efficiency evaluation of RIM framework

The results are presented in TABLE IX. Under the same transmission turnover, we take Case 3d (DIU set) as the baseline, where the pressure drop estimation error is treated as a fixed box. Even without CDR injection, switching from DIU (Case 3d) to DDU (Case 3c) description reduces the total cost, showing that DDU modeling can improve economic efficiency by avoiding overly conservative intraday operation scenarios. Building on this, Case 3a achieves the lowest total cost and the largest economic efficiency improvement of 12.12% relative to the baseline. Although Case

3a incurs a modest day-ahead CDR cost, it substantially reduces intraday electricity cost, resulting in a much better overall cost balance. By contrast, removing the economic regulation rule (Case 3b) leads to the highest total cost, even worse than the no-CDR case (Case 3c), which highlights the necessity of the proposed economic regulation rule to prevent uneconomical operating regimes. Overall, the four-case comparison demonstrates that the proposed framework improves economic efficiency by jointly leveraging DDU modeling and CDR-enabled operation, while maintaining safe transmission.

5.2.4. Workflow Performance Comparison

Comparison terms		**Proposed**	Benders-CCG	Basic C&CG
Case 2	Iterations	**4**	117	2
	Total CPU time (s)	**125.93**	6982.88	127.84
	Objective value (¥)	**21119.42**	21119.42	Infeasible
	Robust feasibility level (MPa)	**0**	0	N/A
Case 3a	Iterations	**3**	182	3
	Total CPU time (s)	**387.63**	86400	64.56
	Objective value (¥)	**151650.44**	N/A	167985.59
	Robust feasibility level (MPa)	**0**	133.67	0

TABLE X Workflow performance

To evaluate the performance of proposed workflow on dealing with DDU sets, other two comparative workflows, i.e., Benders-CCG [28] and basic C&CG-based workflow [26] are both utilized to solve Case 2 and Case 3a. The numerical tests were conducted using YALMIP [41] with Gurobi on the MATLAB R2021b platform, running on an AMD Ryzen 7 5800HS CPU (3.20 GHz) with 16 GB of RAM. The results are recorded in TABLE X. We observe that the proposed workflow successfully solves both cases with rather short time, with the large-scale system taking 387.63s. However, neither Benders-CCG nor basic C&CG-based workflow can stably derive a high-quality feasible solution. Note that the former does not produce a feasible solution for Case 3a after one

day, while the latter one fails to generate feasible solutions in a consistent fashion. Overall, these results verify the stability and efficiency of the proposed workflow in handling scheduling problems considering DDU, highlighting its practical applicability for real-world pipeline operations.

6. Conclusions

This paper proposes a two-stage RIM framework to ensure the security and economic efficiency of STS-RR operation in the energy transition. Specifically, the RIM model considering DDU in pipeline pressure drop within STS-RRs and the solution workflow based on the state-of-the-art parametric C&CG algorithm are proposed. The conclusions are as follows:

1) The proposed IM is essential for ensuring safe and highly economic STS-RR operation while guaranteeing sufficient local demand. The introduction of CDR significantly decreases pressure drop, with a reduction ratio averaging 31.79% for PL2 in Case 1a, thereby reducing electricity costs. For the illustrative case, there is a 22.20% economic improvement in total cost and a 26.08% increase in turnover.
2) The RIM framework further offers practical guidance for on-site dispatchers to safely operate the system corresponding to uncertain pressure drop. Although there is a slight increase in cost compared with the deterministic case, it is negligible when weighed against the benefits of enhanced reliability and reduced infeasibility.
3) Scalability test on the real-world cross-regional refined oil transmission system in South China indicates that, compared with the DIU-only baseline, jointly leveraging DDU modeling and CDR-enabled operation mitigates undue conservatism and achieves a 12.12% improvement in total cost reduction while maintaining secure transmission.
4) The proposed workflow is more efficient and stable in handling scheduling problems,

considering DDU within a reasonable time, highlighting its practical applicability for real-world pipeline operations.

Future work includes generalizing the proposed method to other systems such as the hydrogen-blended natural gas transmission systems.

Acknowledgments

This project was supported by the National Natural Science Foundation of China (52177089 and 52177088), the Fundamental Research Funds for the Central Universities (YCJJ20230463) and PipeChina South China Company (GWHT20200001399).

References

1. IEA. Energy Statistics Data Browser. IEA, Paris. 2023.
2. Li B, Chen Y, Wei W, Wang Z, Mei S. Online coordination of LNG tube trailer dispatch and resilience restoration of integrated power-gas distribution systems. IEEE T SMART GRID. 2022;13:1938-1951.
3. Tu R, Zhang H, Xu S, Fu G, Li Z, Liao Q, et al. Pipeline sharing: Boosting multi-product pipeline transport biofuels in the shift to low-carbon energy. J CLEAN PROD. 2024;437:140663.
4. Wang S, Fang J, Wu J, Liang Y, Ai X, Cui S, et al. Event-triggered security-constrained energy management scheme on shared transmission systems for renewable fuels and refined oil: Implementation and field tests in South China. APPL ENERG. 2025;389:125727.
5. Li Z, Liang Y, Ni W, Liao Q, Xu N, Li L, et al. Pipesharing: economic-environmental benefits from transporting biofuels through multiproduct pipelines. APPL ENERG. 2022;311:118684.
6. Wang S, Fang J, Wu J, Ai X, Cui S, Zhou Y, et al. Learning-based spatially-cascaded distributed coordination of shared transmission systems for renewable fuels and refined oil with quasi-optimality preservation under uncertainty. APPL ENERG. 2025;381:125085.
7. Li Z, Guo Y, Wang B, Yan Y, Liang Y, Mikulčić H. Two-stage optimization model for scheduling multiproduct pipeline network with multi-source and multi-terminal. ENERGY. 2024;306:132511.
8. Liao Q, Liang Y, Xu N, Zhang H, Wang J, Zhou X. An MILP approach for detailed scheduling of multi-product pipeline in pressure control mode. CHEM ENG RES DES. 2018;136:620-637.
9. Li Z, Liao Q, Xu B, Tu R, Li L, Wang Y, et al. A decision-making framework for scheduling of multiproduct pipeline under the fair opening. Journal of Pipeline Science and Engineering. 2024:100185.
10. Wang S, Zuo L, Li M, Wang Q, Xue X, Liu Q, et al. The data-driven modeling of pressure loss in multi-batch refined oil pipelines with drag reducer using long short-term memory (LSTM) network. ENERGIES. 2021;14:5871.
11. Niazi M, Ashrafizadeh SN, Hashemabadi SH, Karami H. CFD simulation of drag-reducing fluids in a non-Newtonian turbulent pipe flow. CHEM ENG SCI. 2024;285:119612.
12. Liu X, Sun W, Chen T, Xu X, Huang T. Energy and environmental performance of iron and steel

industry in real-time demand response: A case of hot rolling process. APPL ENERG. 2025;389:125717.
13. Zhang H, Sun W, Li W, Ma G. A carbon flow tracing and carbon accounting method for exploring CO2 emissions of the iron and steel industry: An integrated material–energy–carbon hub. APPL ENERG. 2022;309:118485.
14. Alsurakji IH, Al-Sarkhi A, El-Qanni A, Mukhaimar A. Experimental insights into energy savings and future directions of drag reducing polymers in multiphase flow pipelines. SCI REP-UK. 2023;13:10619.
15. Li W, Zou Y, Yang H, Fu X, Li Z. Two stage stochastic energy scheduling for multi energy rural microgrids with irrigation systems and biomass fermentation. IEEE T SMART GRID. 2024;16:1075-1087.
16. Li H, Zhang H, Zhang J, Wu Q, Wong C. A frequency-secured planning method for integrated electricity-heat microgrids with virtual inertia suppliers. APPL ENERG. 2025;377:124540.
17. Yan M, Gan W, Zhou Y, Wen J, Yao W. Projection method for blockchain-enabled non-iterative decentralized management in integrated natural gas-electric systems and its application in digital twin modelling. APPL ENERG. 2022;311:118645.
18. Tostado-Véliz M, Jordehi AR, Fernández-Lobato L, Jurado F. Robust energy management in isolated microgrids with hydrogen storage and demand response. APPL ENERG. 2023;345:121319.
19. Bertsimas D, Kim CW. A machine learning approach to two-stage adaptive robust optimization. EUR J OPER RES. 2024;319:16-30.
20. Zhou B, Fang J, Ai X, Zhang Y, Yao W, Chen Z, et al. Partial-dimensional correlation-aided convex-hull uncertainty set for robust unit commitment. IEEE T POWER SYST. 2022;38:2434-2446.
21. Xue X, Fang J, Ai X, Cui S, Jiang Y, Yao W, et al. A fully distributed ADP algorithm for real-time economic dispatch of microgrid. IEEE T SMART GRID. 2023;15:513-528.
22. Jiang W, Wang J, Varbanov PS, Yuan Q, Chen Y, Wang B, et al. Hybrid data-mechanism-driven model of the unsteady soil temperature field for long-buried crude oil pipelines with non-isothermal batch transportation. ENERGY. 2024;292:130354.
23. Wen J, Gan W, Chu C, Jiang L, Luo J. Robust resilience enhancement by EV charging infrastructure planning in coupled power distribution and transportation systems. IEEE T SMART GRID. 2025;16:491-504.
24. Haghighat H, Wang W, Zeng B. Robust unit commitment with decision-dependent uncertain demand and time-of-use pricing. IEEE T POWER SYST. 2023;39:2854-2865.
25. Quan Q, Wang S, Wang L, Shi Y, Xie J, Wang X, et al. Experimental study on the effect of high-molecular polymer as drag reducer on drag reduction rate of pipe flow. J PETROL SCI ENG. 2019;178:852-856.
26. Zeng B, Zhao L. Solving two-stage robust optimization problems using a column-and-constraint generation method. OPER RES LETT. 2013;41:457-461.
27. Chen Y, Wei W. Robust generation dispatch with strategic renewable power curtailment and decision-dependent uncertainty. IEEE T POWER SYST. 2022;38:4640-4654.
28. Zeng B, Wang W. Two-stage robust optimization with decision dependent uncertainty. ArXiv. 2022;abs/2203.16484.
29. Haghighat H, Wang W, Zeng B. Robust microgrid capacity investment with endogenous and exogenous uncertainties. IEEE T SMART GRID. 2023.
30. Wang S, Huang D, Fang J, Ai X, Cui S, Li M, et al. Towards continuous-time safe energy management in shared renewables and refined oil transmission systems. Energy Internet. 2025:e12024.

31. Zhou X, Liang Y, Zhang X, Liao Q, Gao S, Zhang W, et al. A MILP model for the detailed scheduling of multiproduct pipelines with the hydraulic constraints rigorously considered. COMPUT CHEM ENG. 2019;130:106543.
32. Wang S, Fang J, Ai X, Cui S, Zuo L, Li M, et al. Implementation and field test of optimal pump scheduling in the multiproduct refined oil transmission system. IEEE T IND APPL. 2022;58:7930-7941.
33. Shao K, Wang X, Liu M, Xu A, Jian L. Efficient pump scheduling for large-scale multiproduct pipelines using deep reinforcement learning. INT J ADAPT CONTROL. 2024;0:1-13.
34. Dai X, Zhao L, He R, Du W, Zhong W, Li Z, et al. Data-driven Wasserstein distributionally robust chance-constrained optimization for crude oil scheduling under uncertainty. CHINESE J CHEM ENG. 2024;69:152-166.
35. Dai X, Zhao L, He R, Du W, Zhong W, Li Z, et al. Data-driven crude oil scheduling optimization with a distributionally robust joint chance constraint under multiple uncertainties. COMPUT CHEM ENG. 2023;171:108156.
36. Li Z, Liang Y, Liao Q, Xu N, Zheng J, Zhang H. Scheduling of a branched multiproduct pipeline system with robust inventory management. COMPUT IND ENG. 2021;162:107760.
37. Elhafaia MH, Nova-Rincon A, Sochard S, Serra S, Reneaume J. Optimization of the pipe diameters and the dynamic operation of a district heating network using a robust initialization strategy. APPL THERM ENG. 2024:124533.
38. Zhang Y, Ai X, Wen J, Fang J, He H. Data-adaptive robust optimization method for the economic dispatch of active distribution networks. IEEE T SMART GRID. 2019;10:3791-3800.
39. Zhang Y, Liu F, Wang Z, Su Y, Wang W, Feng S. Robust scheduling of virtual power plant under exogenous and endogenous uncertainties. IEEE T POWER SYST. 2021;37:1311-1325.
40. Wang S. Data-for-IML-P-C_sharing-in-manuscript, GitHub, v1; 2024. https://github.com/datasharing4manuscript/Data-for-IML-P-C_sharing-in-manuscript.git.
41. Lofberg J, "YALMIP: A toolbox for modeling and optimization in MATLAB," in 2004 IEEE international conference on robotics and automation (IEEE Cat. No. 04CH37508), (IEEE, 2004), pp. 284-289.